Tailor-Made Macroporous Vanadium Oxide Foams

ARTICLE *in* CHEMISTRY OF MATERIALS · JANUARY 2005

Impact Factor: 8.35 · DOI: 10.1021/cm048554e

Tailor-Made Macroporous Vanadium Oxide Foams

Florent Carn,[†] Nathalie Steunou,[‡] Jacques Livage,*[,‡] Annie Colin,[§] and Rénal Backov*[,†]

Centre de Recherche Paul Pascal, UPR 8641-CNRS, 115 Avenue du Dr Albert Schweitzer, 33600 Pessac, France, Laboratoire de Chimie de la Matière Condensée, UMR-7574 CNRS, 4 Place Jussieu, Université Pierre et Marie Curie, Paris CEDEX 05, France, and Laboratoire du Futur, UMR CNRS-Rhodia FRE2771, IECB, 2 rue Robert Escarpit, 33607 Pessac, France

Received August 30, 2004. Revised Manuscript Received November 9, 2004

Upon a nonstatic patterning method that employs a metastable air−liquid foaming process, macroporous vanadium oxide scaffolds have been synthesized. By controlling the foams liquid fraction, the process in use allows one to tune the size and shape (from spherical to a more polygonal aspect) as well as the Plateau-borders thickness of the vanadium oxide macroscopic void spaces. XRD experiments reveal the amorphous character of the vanadium oxide matrices intercalated with surfactant entities, while the local structure around vanadium atoms, as demonstrated with ^{51}V NMR MAS experiments, is close to that obtained for V_2O_5 xerogel.

Introduction

There has been extensive interest toward organic−inorganic hybrid vanadium oxides mainly for their structural diversity and potential applications in various domains as, for instance, heterogeneous catalysis, cathodic materials for advanced lithium batteries, visible light photochromism, and electrochromic devices.[1,2] This particular interest, beyond the structural and electronic properties, is certainly enhanced by the fact that aqueous V_2O_5 gels are one of the best examples of materials synthesized upon the "sol−gel process"[3,4] with the capability of shaping and organizing the inorganic polymer through the process of "chimie douce", that is, soft chemistry.[5] Those syntheses allow one to reach either hybrid organic−inorganic materials where the properties are coming from each constituent[6,7] or inorganic gels where nematic liquid crystals are obtained under specific synthetic and aging time conditions; that is, a high anisotropy aspect ratio of V_2O_5 ribbons enhances the high-scale organization.[8−10] In this last issue of high-scale organization and taking a more general context of "chemistry of shapes"[11] or synthesis over "all length scale",[12] macroporous crystalline vanadium oxide foam has been produced via an effervescence method without providing a strong control over macroscopic cell morphologies.[13] With this study, we present an alternative method that combines soft matter used as a macroscopic pattern taking benefit of bubbling air−liquid foaming systems and soft chemistry to generate the inorganic polymer. As was previously demonstrated for silica[14] or titanium dioxide,[15] this method allows a complete control over the bubble cell sizes and shapes, working easier with the foams liquid fraction and with the glass pore sizes employed during the bubbling process. The final monolith-type materials depict macroscale void spaces where, for the first time, macroscale vanadium oxide cell morphologies, that is, length, width, and curvature of the Plateau borders, can be tuned with a strong degree of control.

Experimental Section

Macroporous Vanadium Oxide Foams Syntheses. Dowex 50WX2-100 ion-exchange resin and sodium metavanadate (90%) were purchased from Aldrich. Tergitol type NP-10 was purchased from Sigma. The perfluoro-compound FC72 was purchased from Across Organics.

The synthesis of $V_2O_5 \cdot nH_2O$ gels was performed by the ion-exchange method.[3,16,17] A solution of a sodium metavanadate ($NaVO_3$) precursor of concentration 0.1 mol/L was passed through a proton exchange resin (DOWEX-W-hydrogen, strongly acidic cation, 2% cross-linking 50−100 mesh). As acidification occurs, the pH of the solution decreased from 7 to 2.6. At a pH close to 2.6, the solution started to polymerize, and, after 20 h, a dark red gel of V_2O_5 ribbons formed. The vanadium weight fraction in this gel was determined by preparing a dry extract.

* Corresponding authors. (R.B.) Phone: 33 (0)5 56 84 56 30. Fax: 33 (0)5 56 84 56 00. E-mail: backov@crpp-bordeaux.cnrs.fr. (J.L.) Phone: 33 (0)1 44 27 33 65. Fax: 33 (0)1 44 27 47 69. E-mail: livage@ccr.jussieu.fr.

[†] Centre de Recherche Paul Pascal.

[‡] Université Pierre et Marie Curie.

[§] Laboratoire du Futur.

(1) Baker, L. C. W.; Glick, D. C. *Chem. Rev.* **1998**, *98*, 3.
(2) Hagrman, P. J.; Finn, R. C.; Zubieta, J. *Solid State Sci.* **2001**, *3*, 745.
(3) Livage, J. *Chem. Mater.* **1991**, *3*, 578.
(4) Brinker, C. J.; Scherer, G. W. *Sol−Gel Science: the Physics and Chemistry of Sol−Gel Processing*; Academic Press: San Diego, 1990.
(5) Livage, J. *New J. Chem.* **2001**, *25*, 1.
(6) Kanatzidis, M. G.; Wu, C.-G. *J. Am. Chem. Soc.* **1989**, *111*, 4139.
(7) Leroux, F.; Kœne, B. E.; Nazar, L. F. *J. Electrochem. Soc.* **1997**, *144*, 3886.
(8) Zocher, H. *Z. Anorg. Allg. Chem.* **1925**, *147*, 91.
(9) Davidson, P.; Garreau, A.; Livage, *J. Liq. Cryst.* **1994**, *16*, 905.
(10) Livage, J.; Pelletier, O.; Davidson, P. *J. Sol.-Gel Sci. Technol.* **2000**, *19*, 275.
(11) Mann, S. *Nature* **1993**, *365*, 499.
(12) Soten, I.; Ozin, G. A. *Curr. Opin. Colloid Interface Sci.* **1999**, *4*, 325.
(13) Chandrappa, G. T.; Steunou, N.; Livage, J. *Nature* **2002**, *416*, 702.
(14) Carn, F.; Colin, A.; Achard, M.-F.; Deleuze, H.; Backov, R. *Adv. Mater.* **2004**, *16*, 140.
(15) Carn, F.; Colin, A.; Achard, M.-F.; Deleuze, H.; Sanchez, C.; Backov, R. *Adv. Mater.* **2005**, *17*, 68.
(16) Pelletier, O.; Davidson, P.; Bourgaux, C.; Coulon, C.; Regnault, S.; Livage, J. *Langmuir* **2000**, *16*, 5295.
(17) Vigolo, B.; Zakri, C.; Nallet, F.; Livage, J.; Coulon, C. *Langmuir* **2002**, *18*, 9121.

10.1021/cm048554e CCC: $30.25
Published on Web 01/13/2005

Foaming solutions were prepared by mixing a nonionic surfactant, water, and $V_2O_5 \cdot nH_2O$ gel. Typically, a $V_2O_5 \cdot nH_2O$ gel was added to an aqueous solution of Tergitol NP10 (10 wt %) to reach a proportion of 65 wt %. At this stage, the pH of the sol remained at the value of 2.8. The previous mixture was submitted to a strong stirring during 30 min to homogenize the solution.

Foams were obtained by bubbling perfluorohexane saturated with nitrogen through a porous glass disk (porosity: 100−160, 40−100, 16−40, 10−16 μm) into the foaming solution. The reaction took place inside the Plexiglas column. To minimize the foam destabilization by the drainage (i.e., the gravity-induced liquid flow between bubbles), we chose to wet the foam from above with the sol solution. A stationary regime was reached, and the amount of solution injected at the top of the foam compensated for the amount of liquid evacuated at the bottom. This strategy allowed us to prepare foams with homogeneous liquid fraction from the top to the bottom of the column. We recalled that the liquid fraction (ρ) is the ratio of the volume of liquid present in the foam divided by the total volume of the foam. This technique permitted us to tune the liquid fraction by varying the flux of sol at the foam's top (Q). High flux induced high liquid fractions. The foam's liquid fraction can be checked using conductivity measurements. Metastable foams were recuperated at the top of the column with a spatula and stocked into a beaker. Final foams were then frozen overnight at −80 °C and lyophilized during 5 h.

Resulting hybrid organic−inorganic monolith-type materials were then either washed with THF for 48 h to remove the surrounding surfactant or thermally treated at 600 °C to both calcine all of the surfactant and enhance V_2O_5 crystallization/oxidation. The temperature increase was monitored at 2 °C min^{-1} with a first plateau at 200 °C for 2 h. The cooling process was uncontrolled and directed by the oven inertia.

Characterization. TEM experiments were performed with a JEOL 2000-FX microscope (accelerating voltage of 200 kV). The samples were prepared as follows: vanadium oxide foams in a powder state were deposited on a copper grid coated with a Formvar membrane. SEM observations were performed with a JEOL JSM-840A scanning electron microscope operating at 10 kV. The specimens were carbon-coated prior to examination. Thermogravimetric analyses were carried out under an oxygen flux of 5 cm^3 min^{-1} at a heating rate 5 °C min^{-1} using a Setaram TAG-1750 thermogravimetric analyzer. XRD experiments were carried out with an X'pert MPD Philips using Cu Kα radiation and an average current of 50 mA. EPR measurements were recorded at room temperature on a Bruker ESP 300E X-band spectrometer with 100 kHz modulation, and DPPH was used as an external standard. Solid-state ^{51}V MAS NMR spectra were performed at 79.0 MHz on a Bruker Avance 300 spectrometer using a MAS 4 mm ^{1}H/BB probe. Solid samples were spun at 14 kHz using 4-mm ZrO_2 rotors. ^{51}V MAS NMR spectra were acquired with a Hahn echo sequence ($\pi/2-\tau-\pi-\tau$ acquisition) with a synchronized τ and a 16 phases pulse program. The following acquisition parameters were used: spectral width of 1 MHz, pulse width of 2 μs, and 0.5 s of recycle time. An accumulation of 14 000 transients was usually performed on each sample. Isotropic chemical shifts are referenced to pure $VOCl_3$ using a solution of 0.5 mol L^{-1} $NaVO_3$ ($\delta_{iso} = -578$ ppm). Numerical simulations of the ^{51}V MAS spectra were performed with QUASAR.[18] These simulations included the effects of the chemical shift anisotropy (CSA) as well as the first- and second-order quadrupolar interactions; both central and satellite transitions were considered.

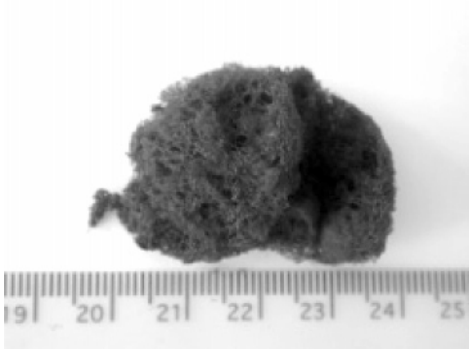

Figure 1. Vanadium oxide foam obtained as monolith.

Results and Discussion

Macroscopic Shaping. The method employed for this study induces formation of vanadium oxide foams as the monoliths state (Figure 1). Upon the nonstatic method developed during the course of our previous study,[14,15] we succeeded in controlling macroscopic cell morphologies of vanadium oxide foam by working with the starting air−liquid foam liquid fractions (ρ) and the bubbling apparatus pore size.

The foam liquid fraction is controlled via the sol flux (Q) imposed at the top of the foam (see Experimental Section). The relationship between ρ and the foam morphology can be expressed with the following equation:[19]

$$\rho = 0.171(r/L_{PB})^2 + 0.256(r/L_{PB})^3 \approx a/L_{PB}{}^2 * [\,1 + 3.98(a/L_{PB}{}^2)^{1/2}]$$

where "r" is the Plateau-borders curvature, "L_{PB}" is the Plateau-borders length, and "a" is the Plateau-borders width. The foam liquid fraction ρ can be tuned by varying the sol flux (Q) at the top of the foam. Using this drainage property, either polygonal (Figure 2a and b) or spherical (Figure 2c and d) vanadium oxide macroscopic cell morphologies can be obtained, respectively, for low liquid fraction and high liquid fraction. As far as the foam's liquid fraction can vary, beyond cell shapes, Plateau-border thickness can be controlled. In this issue, both the hybrid (noncalcined foam, Figure 2a and c) and the inorganic (calcined, Figure 2b and d) vanadium oxide cell border thicknesses are varying upon the sol flux applied at the top of the starting air−liquid foams. This feature is also observed when the hybrid foams are washed (Figure 2e) with THF. If we focused on Figure 2b, d, and e, it is noticeable that the hybrid scaffolds endure a strong shrinkage during the THF washing treatment, shrinkage enhanced when thermal treatment is applied. This shrinkage induced by the thermal treatment is higher (around 65%) when compared to the one associated with SiO_2 (around 30%),[14] whereas it appears similar to the shrinkage effect associated with TiO_2 (around 50%).[15] In fact, for the vanadium oxide as for titanium dioxide, this high shrinkage is certainly enhanced both by the sintering effect and by the inorganic scaffold crystallization. This crystallization aspect and the organic-part removal will be discussed later in the text.

(18) Amoureux, J. P.; Fernandez, C.; Dumazy, Y. *37th Rocky Mountain Conference*; Abstract no 264; Denver, 1995 (program accessible within Dmfit 2004 Version at the following URL address: http://crmht-europe.cnrs-orleans.fr/dmfit/help/dmfit.htm).

(19) Phelan, R.; Weaire, D.; Peters, E. A. J. F.; Verbist, G. *J. Phys.: Condens. Matter* **1996**, *8*, 475.

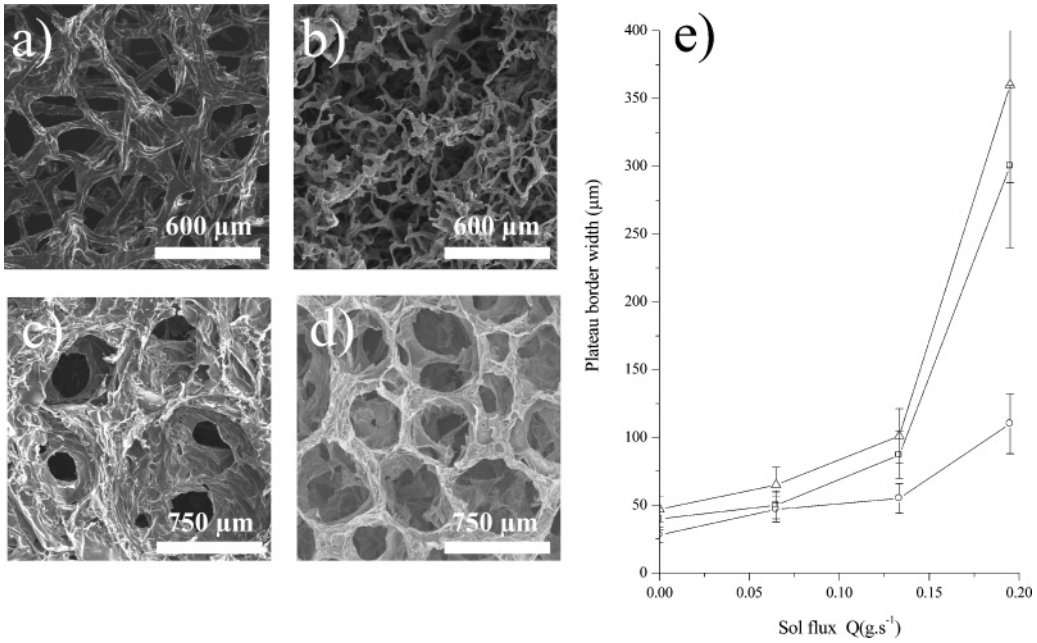

Figure 2. Vanadium oxide foams. Evolution of the Plateau-borders width with the flux conditions Q, using the same porous glass disk of 70 μm pores diameter: (a) SEM image of a V_2O_5−Tergitol(NP10) foam (before calcination) obtained without wetting ($Q = 0$ g s^{-1}), (b) SEM image of the same monolith after thermal treatment at 600 °C, (c) SEM image of a V_2O_5−Tergitol(NP10) foam (before calcination) obtained with $Q = 0.195$ g s^{-1}, (d) SEM image of the same monolith after thermal treatment at 600 °C, and (e) evolution of the Plateau-borders width as a function of Q (△, before surfactant removal; □, after THF washing; ○, after thermal treatment).

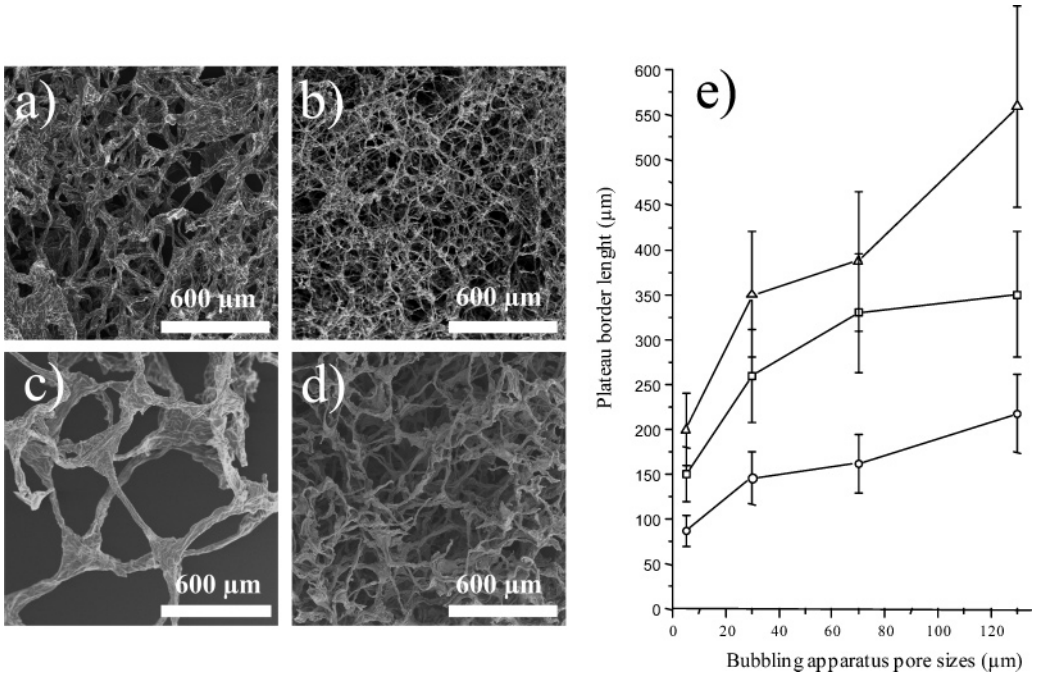

Figure 3. Vanadium oxide foams. Control over the Plateau-borders length by varying the porous disk used during the bubbling and without wetting ($Q = 0$ g s^{-1}): (a) SEM image of a V_2O_5−Tergitol(NP 10) foam (before calcination) obtained from disk with 70 μm pores diameter, (b) SEM image of the same monolith after thermal treatment at 600 °C, (c) SEM image of a V_2O_5−Tergitol(NP10) foam (before calcination) obtained from disk with 130 μm pores diameter, (d) SEM image of the same monolith after thermal treatment at 600 °C, and (e) evolution of the Plateau-borders length with the bubbling apparatus pore sizes (△, before surfactant removal; □, after THF washing; ○, after thermal treatment).

To tune the average macroscopic cell diameters, we varied the porous disk diameter employed at the bottom of the column during the bubbling process (Figure 3). We observed that the Plateau-border lengths, defined as the node-to-node distance, can vary from 200 to 550 μm for the hybrid foams and decrease to 100 and 300 μm when washed with THF and dried, to reach the range of 60−200 μm when thermal treatment is applied. This result demonstrates that, as for the Plateau-border widths, the Plateau-border lengths are also subject to a strong shrinkage effect (Figure 3e).

Effect of THF Washing, Thermal Treatments, and Associate Stoichiometries. To appreciate the amount of organic entity embedded within the inorganic core, we performed some thermogravimetric analysis (TGA) measurements (Figure 4) in air. Thermogravimetric analysis associated with the V_2O_5·NP10·nH$_2$O reveals three successive

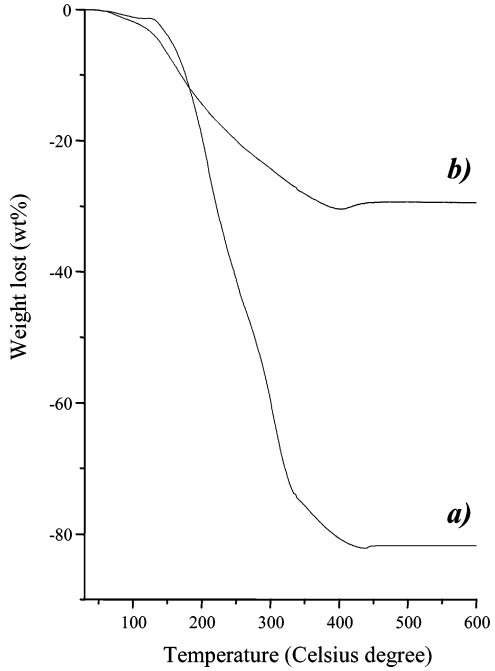

Figure 4. TGA curves obtained under O_2 gas flow: (a) $[(NP10)_{1,19}\cdot 0.52H_2O]/[V_2O_5\cdot(NP10)_{0,14}\cdot 0.12H_2O]$ foam, (b) $[(NP10)_{1,19}\cdot 0.52H_2O]/[V_2O_5\cdot(NP10)_{0,14}\cdot 0.12H_2O]$ foam washed 48 h in THF.

weight losses (Figure 4a). The first weight loss of 1.2% observed from 30 to 130 °C should be induced by the departure of adsorbed water molecules. The last two weight losses correspond to the organic groups decomposition. The approximate stoichiometry deduced from this TGA analysis is $V_2O_5\cdot(NP10)_{1,33}\cdot 0.64H_2O$. The weight loss of 73% between 130 and 340 °C could be associated with the surfactant envelop elimination coexisting with the loss of water confined within vanadium oxide layers. The final weight loss of 7.9%, arising from 340 to 430 °C, could be assigned to the intercalated surfactant removal. According to this explanation, the unwashed composite can be associated with the following stoichiometry: $[(NP10)_{1,19}\cdot 0.52H_2O]/[V_2O_5\cdot(NP10)_{0,14}\cdot 0.12\ H_2O]$, where $[(NP10)_{1,19}\cdot 0.52H_2O]$ corresponds to the surrounding organic part and $[V_2O_5\cdot(NP10)_{0,14}\cdot 0.12H_2O]$ is related to the hybrid assembly of surfactant intercalated within the vanadium oxide interlayer gallery. Above 450 °C, we can observe a weight gain certainly related to vanadium oxide species oxidation toward V_2O_5 generation and crystallization.[20] The TGA curve of the composite materials washed during 48 h in THF (Figure 4b) depicts a two-step weight loss. The first 1.8% water weight loss at 130 °C is followed by an organic weight loss of 28% until 400 °C. The stoichiometry associated with this washed sample is $V_2O_5\cdot(NP10)_{0,12}\cdot 0.12H_2O$. This result is consistent with the composite compound stoichiometry suggested previously: $[(NP10)_{1,19}\cdot 0.52H_2O]/[V_2O_5\cdot(NP10)_{0,14}\cdot 0.12H_2O]$, where the surrounding organic part of the composite is being washed under THF treatment. As was previously observed, a weight gain is observed at 450 °C due to the same vanadium oxide oxidation/crystallization phenomenon.

XRD and Microstructure. The $[(NP10)_{1,19}\cdot 0.52H_2O]/[V_2O_5\cdot(NP10)_{0,14}\cdot 0.12\ H_2O]$ X-ray diffraction pattern (Figure 5b) reveals overall a noncrystalline character with two broad peaks at low angles $2\Theta = 5.16°$ ($d_{001} = 17.12$ Å) and $2\Theta = 9.70°$ that can be assigned to the 001 and 002 harmonic peaks characteristic of a lamellar phase. A strong and broad diffraction peak centered at $2\Theta = 20°$ is related to the poor intrinsic organization of the surfactant when compared to the pure Tergitol diffraction pattern (Figure 5a). The 001 distance is much larger than the distance between vanadium oxide planes in crystalline powder or even when compared to $V_2O_5\cdot 1.6H_2O$ xerogels ($d = 11.50$ Å).[3,21] According to the basal distance of 17.12 Å and taking in account the sheet thickness. we might suggest a configuration where the alkyl chains ($d_{calc}(C_9H_{19}\cdot C_6H_4\cdot(OC_2H_4)_9\cdot OH) = 16.7$ Å) are tilted with an angle of 31° toward the normal of the oxide planes while the hydrophilic chains are adsorbed onto vanadyl surface groups though hydrogen-bond interactions (Scheme 1).[22] The X-ray diffraction pattern of the THF washed compound (Figure 5c) is in good agreement with TGA experiments. The NP10 broad diffraction peak vanishes almost completely, whereas the 001 peak does not vary, thus suggesting that guest entities remain with the same configuration within the interlayer host gallery. The intercalated surfactant removal is reached by calcination at 650 °C. Moreover, the thermal treatment enhances the crystalline character of the vanadium oxide microstructure (Figure 5d). This last X-ray diffraction pattern (Figure 5d) is strongly related to commercial V_2O_5

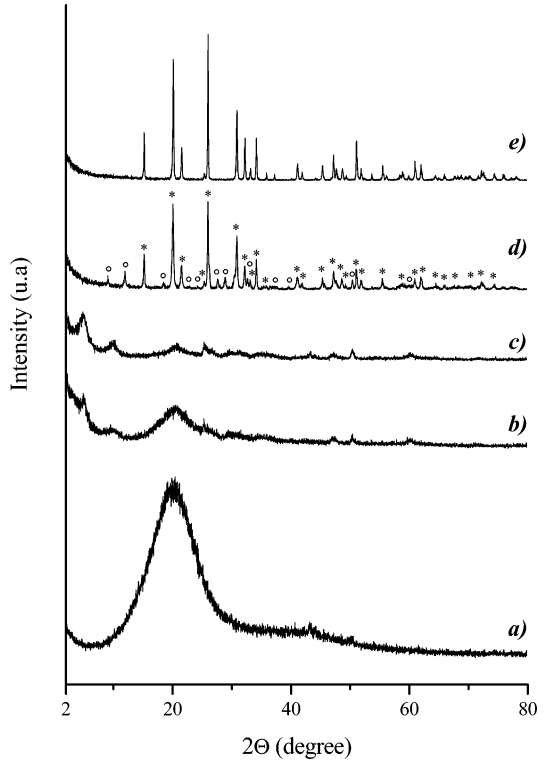

Figure 5. X-ray diffraction patterns of: (a) commercial Tergitol (NP10) surfactant in a liquid state, (b) $[(NP10)_{1,19}\cdot 0.52H_2O]/[V_2O_5\cdot(NP10)_{0,14}\cdot 0.12H_2O]$ foam, (c) $[(NP10)_{1,19}\cdot 0.52H_2O]/[V_2O_5\cdot(NP10)_{0,14}\cdot 0.12H_2O]$ foam washed during 48 h using THF, (d) $[(NP10)_{1,19}\cdot 0.52H_2O]/[V_2O_5\cdot(NP10)_{0,14}\cdot 0.12H_2O]$ foam after thermal treatment at 600 °C, and (e) commercial V_2O_5 powder. ∗, commercial V_2O_5;[23a] °, commercial NaV_6O_{15}.[23b]

(20) Bouhedja, L.; Steunou, N.; Maquet, J.; Livage, J. *J. Solid State Chem.* **2001**, *162*, 315.

(21) Aldebert, P.; Baffier, N.; Gharbi, N.; Livage, J. *Mater. Res. Bull.* **1981**, *16*, 669.

(22) Fontenot, C. J.; Wiench, J. W.; Schrader, G. L.; Pruski, M. *J. Am. Chem. Soc.* **2002**, *124*, 8435.

Scheme 1. Hypothesized Orientation of the Tergitol NP10 Chains (C_9H_{19}·C_6H_4·$(OC_2H_4)_9$·OH) within Vanadium Oxide Layers Deduced from X-ray Diffraction Patterns

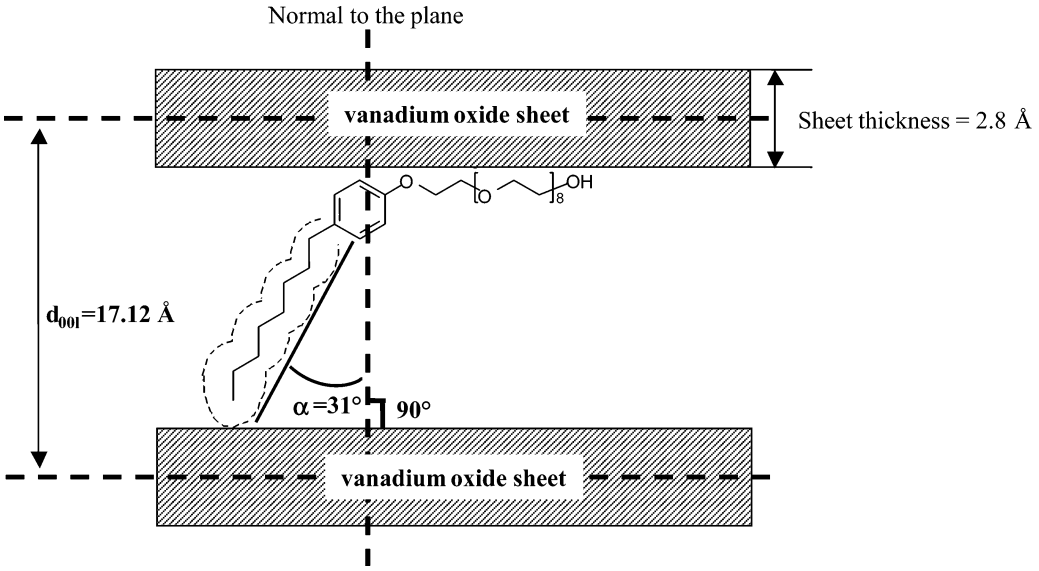

[23a] (Figure 5e) with additional diffraction peaks that correspond to NaV_6O_{15},[23b] meaning that some residual $Na(VO_3)$ is still present through the proton resin exchange process.

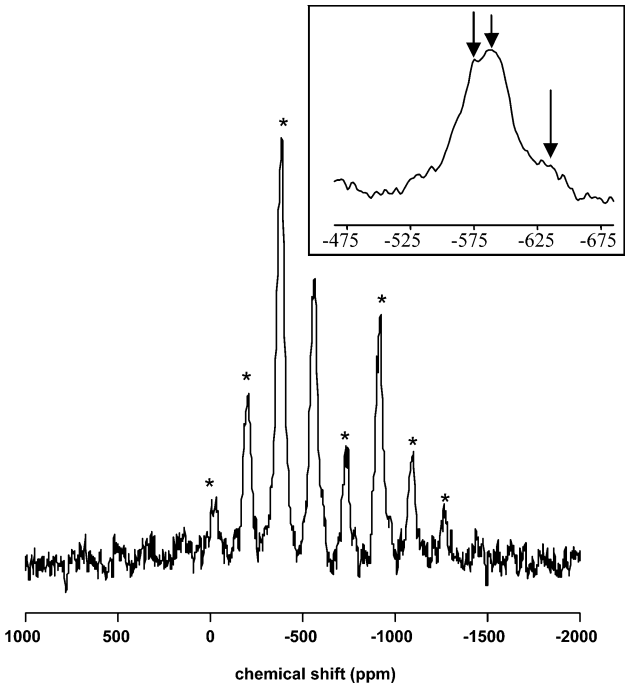

Figure 6. ^{51}V MAS NMR spectrum of the hybrid vanadium oxide foam RO = 14 kHz, NS = 14 000. ∗: spinning sidebands; magnification of the isotropic resonances in the inset.

^{51}V MAS NMR. Considering the THF washed materials and despite the amorphous character, it seems important to estimate the local order around the vanadium atoms and compare it to V_2O_5. In this issue, we performed some solid-state ^{51}V NMR MAS experiments on the composite and THF washed vanadium oxide foams. Both compounds exhibit similar ^{51}V NMR spectra. Figure 6 displays a ^{51}V MAS NMR spectrum of the hybrid vanadium oxide foam, which is quite close to that of a V_2O_5·$1.6H_2O$ xerogel. Deconvolution and integration of the signals intensities including the spinning sidebands indicate the presence of three isotropic resonances at −576, −593, −630 ppm with a relative distribution of 35%, 52%, and 13%. For the two main resonances at −576 and −593 ppm, it was possible to perform a simulation of the spinning sidebands patterns including the effect of the chemical shift anisotropy (CSA) as well as first- and second-order quadrupolar interactions. The parameters obtained are consistent with those obtained for the signals assigned, respectively, to the V_5 and V_2+V_4 sites previously reported for V_2O_5·$1.6H_2O$ xerogel (Scheme 2).[24] The V_5 site corresponds to a square pyramid VO_5 environment with a water molecule trans to the vanadyle V=O bond. The V_2 site corresponds to a highly distorted VO_5 environment, and the V_4 site corresponds to a square pyramid VO_5 environment

Scheme 2. Different Solid-State ^{51}V NMR MAS Sites (Mainly Extracted from Ref 22)

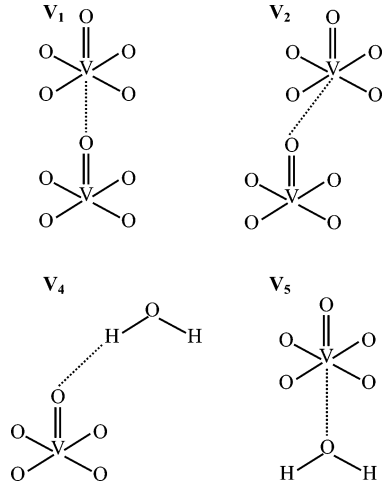

(23) (a) Schulz, D.; Larson, F.; McCarthy, G. ICDD Grant-in-Aid, North Dakota State University, Fargo, ND, 1988. (b) Wadsley, A. D. *Acta Crystallogr.* **1955**, *8*, 695.

(24) Fontenot, C. J.; Wiench, J. W.; Pruski, M.; Schrader, G. L. *J. Phys. Chem. B* **2001**, *105*, 10496.

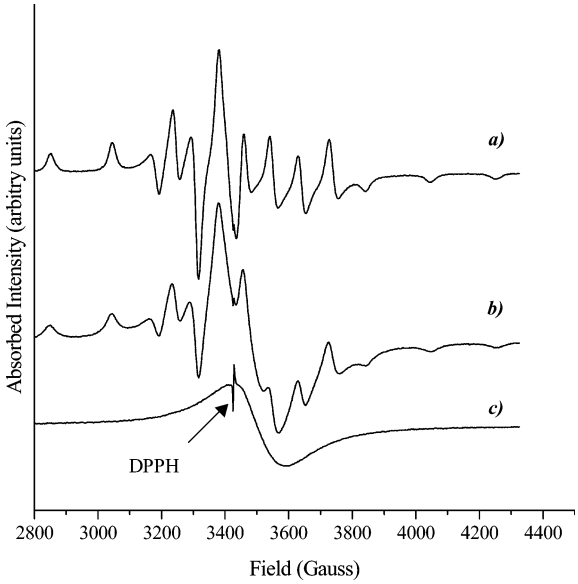

Figure 7. EPR spectrum of the vanadium oxide foams: (a) unwashed sample, (b) washed with THF, and (c) thermally treated at 600 °C.

with a water molecule interacting with the vanadyle bond.[22,24] The signal at −630 ppm is quite broad. This important line width may be attributed to a chemical shift distribution, indicating a structural disorder in the vanadium environment. Moreover, this signal cannot be assigned unambiguously because its important line width and poor intensity prevent an accurate determination of the CSA and quadrupolar parameters. However, as its chemical shift is quite close to that of the V_1 site in $V_2O_5 \cdot 1.6H_2O$ xerogel (−620 ppm), this signal may correspond to the local V_1 site environment, which is close to the square pyramid environment of vanadium in crystalline V_2O_5. In contrast to the spectrum of the $V_2O_5 \cdot 1.6H_2O$ xerogel, the resonance at −663 ppm is not present in the vanadium oxide foam, but in the xerogel this resonance contributes to almost 6% of the total signal intensity.

EPR Spectroscopy. The presence of V(IV) ($3d^1$) paramagnetic species has been detected via EPR spectroscopy (Figure 7). The average Lande factors calculated from the EPR spectrum are 1.99, 1.97, and 1.96, respectively, for the composite foams, hybrid foams washed, and foams treated at 600 °C that correspond to typical g_{av} values observed for vanadium oxides materials.[25] For the unwashed and THF washed compounds, hyperfine structure lines can be observed emerging from the interaction of the unpaired electron with the ^{51}V nucleus.[25] In the case of the thermally treated foams, hyperfine structures are vanished meaning that the interactions are certainly dominated by the magnetic dipolar interaction mechanism.[26]

Conclusion

We have prepared macroporous vanadium oxide foams where at the macroscopic length scale Plateau-border lengths, widths, and shapes can be tuned with a strong degree of control. The vanadium oxide foams, at the microscopic level, depict an amorphous character with a local order, around the vanadium atoms, close to that of V_2O_5 xerogel. Thermal treatment enhanced those materials' crystalline character. The fact that those vanadium oxides' architectures are obtained in a monolith state is also an important feature toward potential applications in heterogeneous catalysis, rechargeable batteries, humidity sensors, and electrochromic devices.

Acknowledgment. We thank Jocelyne Maquet for her help in the solid-state NMR spectra acquisition and Xavier Le Goff for the EPR spectrum acquisition. This work is part of the 6th PCRDT-FAME-MIOH program.

CM048554E

(25) Dyrek, K.; Adamski, A.; Sojka, Z. *Spectrochim. Acta, Part A* **1998**, *54*, 2337.
(26) Chopra, N.; Mansingh, A. *J. Non-Cryst. Solids* **1992**, *146*, 261.